

This is a self-archived version of an original article. This version may differ from the original in pagination and typographic details.

Author(s): Rusanen, Annu; Lahti, Riikka; Lappalainen, Katja; Kärkkäinen, Johanna; Hu, Tao; Romar, Henrik; Lassi, Ulla

Title: Catalytic conversion of glucose to 5-hydroxymethylfurfural over biomass-based activated carbon catalyst

Year: 2020

Version: Accepted version (Final draft)

Copyright: © 2019 Elsevier B.V. All rights reserved.

Rights: CC BY-NC-ND 4.0

Rights url: <https://creativecommons.org/licenses/by-nc-nd/4.0/>

Please cite the original version:

Rusanen, A., Lahti, R., Lappalainen, K., Kärkkäinen, J., Hu, T., Romar, H., & Lassi, U. (2020). Catalytic conversion of glucose to 5-hydroxymethylfurfural over biomass-based activated carbon catalyst. *Catalysis Today*, 357, 94-101. <https://doi.org/10.1016/j.cattod.2019.02.040>

1 Catalytic conversion of glucose to 5-hydroxymethylfurfural over biomass-based
2 activated carbon catalyst

3 Annu Rusanen^a, Riikka Lahti^{a,b}, Katja Lappalainen^{a,b}, Johanna Kärkkäinen^a, Tao Hu^a, Henrik Romar^a, Ulla
4 Lassi^{*,a,b}

5
6 ^a University of Oulu, Research Unit of Sustainable Chemistry, P.O. Box 4300, FIN-90014 Oulu, Finland

7 ^b University of Jyväskylä, Kokkola University Consortium Chydenius, Talonpojankatu 2B, FIN-67100 Kokkola, Finland

8
9 *Corresponding author: ulla.lassi@oulu.fi

10

11

12 **Abstract**

13 Selective and efficient dehydration of glucose to 5-hydroxymethylfurfural (HMF) has been widely explored
14 research problem recently, especially from the perspective of more sustainable heterogeneous catalysts. In
15 this study, activated carbon was first produced from a lignocellulosic waste material, birch sawdust. Novel
16 heterogeneous catalysts were then prepared from activated carbon by adding Lewis or Brønsted acid sites
17 on the carbon surface. Prepared catalysts were used to convert glucose to HMF in biphasic water:THF
18 system at 160 °C. The highest HMF yield and selectivity, 51% and 78%, respectively, were obtained in 8
19 hours with a catalytic mixture containing both Lewis and Brønsted acid sites. Also, preliminary recycling
20 experiments were performed. Based on this study, biomass-based activated carbon catalysts show promise
21 for the conversion of glucose to HMF.

22

23 **Keywords**

24 Activated carbon; Catalyst; 5-hydroxymethylfurfural; Glucose conversion

25

26

27 1. Introduction

28

29 The limitations of fossil resources have driven global society toward bioeconomy, in which bioresources are
30 utilized in the production of biofuels and biochemicals. 5-hydroxymethylfurfural (HMF), a top value-added
31 biomass-derived chemical, has emerged as an important target product, since it represents a potential
32 substitute for petroleum-based monomers of various polymers and can be used as a starting material for
33 biofuels, solvents, and pharmaceuticals [1, 2]. HMF is a heterocyclic furanic molecule substituted in 2–5
34 positions with hydroxide and aldehyde functionalities (Figure 1), making it capable oxidizing into a
35 dicarboxylic acid or reducing to a diol, both of which can be used for the synthesis of polymers. In addition,
36 as a relatively unsaturated aromatic compound, HMF can be upgraded to a fuel *via* hydrogenation, and the
37 heterocyclic structure of furans can be found in an array of biologically active molecules with
38 pharmaceutical applications. [3]

39 HMF can be produced by the dehydration of C6 carbohydrates, including monomeric and polymeric
40 carbohydrates, such as fructose, glucose, sucrose, starch, cellulose, and raw biomass. The mechanistic
41 pathway of transformation is not yet clear, although a few possible alternatives have been proposed [4].
42 The most widely discussed route, when using fructose as feedstock, is direct dehydration of hexoses into
43 HMF, *via* either an acyclic or cyclic intermediate [5, 6]. When using hexoses other than fructose,
44 isomerization has been proposed as an initial step prior to dehydration (Figure 1) [4]. Because of this extra
45 step, the typical yields of HMF from fructose are superior to those obtained from glucose or other hexoses
46 under the same reaction conditions. Up to 99% yields have already been achieved in fructose conversion to
47 HMF [7]. Still, it should be emphasized that fructose is not an ideal feedstock because of its high price and
48 low abundance in nature [8]. It exists only in food biomass, such as in sugar cane or corn; in contrast,
49 glucose is the cheapest hexose and the most abundant monosaccharide, and is also available in non-food
50 lignocellulosic biomass. Therefore, the conversion of glucose to HMF is an important challenge worthy of
51 study.

52 There are many ways to produce HMF from glucose—for example, aqueous, organic, biphasic and
53 ionic liquid systems have all been utilized recently [4]. When compared to fructose conversion systems, the
54 challenge with glucose conversion is to find media wherein a rather stable glucose pyranose can transfer
55 effectively into a furanose form. Also, the low selectivity of the dehydration reaction, which is caused by
56 multiple side reactions, such as the formation of undesired byproducts, lowers the yield [9]. Formic acid
57 and levulinic acid can be formed *via* the rehydration of HMF [10]. Also, a cross-polymerization reaction
58 leads to the formation of soluble polymers and insoluble brown humins [11]. Biphasic systems are
59 promising media for conversion since the separation of HMF is simple and the system is recyclable, while
60 yields remain good (up to 81% in THF/water/NaCl system) [12, 13]. The most remarkable advantage of the
61 biphasic system is the continuous removal of HMF from the reaction mixture, which prevents rehydration
62 reactions and increases yields. DMSO:water, MIBK:water, and THF:water are the most-used biphasic
63 systems according to the literature [4, 14].

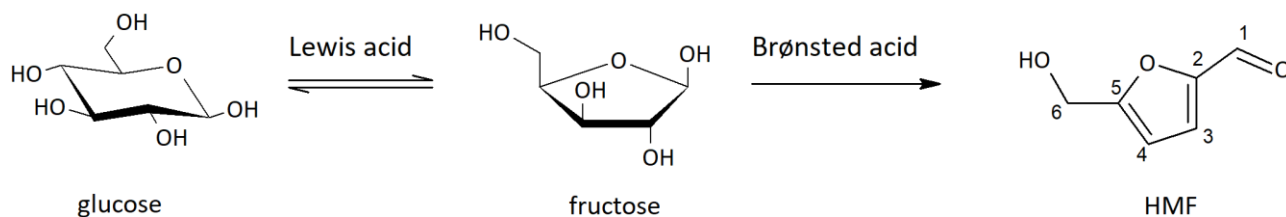
64 In addition to reaction media, the catalyst also plays an important role in reaction selectivity and
65 the dehydration rate. The dehydration step is generally catalyzed by mineral or organic acid. The catalyst
66 should either possess a proton or be a Lewis acid [15, 16]. The most commonly used Brønsted acids are
67 sulfuric acid, phosphoric acid, hydrochloric acid, oxalic acid, levulinic acid, and p-toluenesulfonic acid [4].
68 The isomerization step is catalyzed by Brønsted bases or Lewis acids [17]. However, the basic catalyst
69 typically leads to side reactions, so Lewis acids, such as metal chlorides, are favored [18]. Homogeneous
70 metal chlorides are capable of producing good HMF yields from glucose, e.g., AlCl₃ produced a 61% yield in
71 the biphasic system at 160 °C [19]. Also, tandem systems, in which the presence of both Lewis and

72 Brønsted acidity are combined, have been used, e.g., AlCl₃ and HCl as a tandem system produced a 62%
73 yield in the biphasic system at 170 °C [20].

74 However, traditional homogeneous catalysts are not easily recycled, they cause corrosion and incur
75 significant costs in separation and waste treatment processes. Heterogeneous catalysts, on the other hand,
76 are easily separated from the liquid reaction mixture after the reaction, enabling their reuse. Therefore, the
77 replacement of homogeneous catalysts with heterogeneous catalysts is preferred and is currently drawing
78 attention in the research field [21]. The most commonly used heterogeneous acid catalysts include metal
79 oxides, functional polymers, ion exchange resins, and zeolites [22-25]. As an alternative to them, novel
80 heterogeneous catalysts can be prepared from activated carbons (AC). ACs are low-cost materials
81 possessing large specific surface areas, well-developed, highly porous structures, chemical and physical
82 stability, and surface functionalities influencing the surface characteristics and adsorption behavior. ACs
83 can be inert or active in reactions. The carbon materials exhibit an acid–base character by containing
84 heteroatom, such as oxygen-bearing surface groups, which can have an effect on its properties. [26-29]
85 Furthermore, AC can be used as a catalyst support and be chemically functionalized and/or impregnated
86 with metals to improve catalytic activity [30-32]. ACs can be prepared from any carbon-containing raw
87 material, including bituminous coal and lignite, from which a large part of the ACs on the market is
88 produced [33]. Biomass-based ACs [34-36] are becoming more attractive, since they can be prepared from
89 lignocellulosic second-generation biomasses, side streams, and waste materials as a renewable raw
90 material, and as such contribute to carbon neutrality in the face of climate change.

91 Recently, a few studies have been published about fructose conversion to HMF by using modified
92 carbon catalysts: Deng et. al. used sodium ligninsulfonate derived AC as a catalyst support functionalized
93 with phosphoric acid, whereas Xiong et. al. used wood-based forestry biochar sulfonated with sulfuric acid
94 [37, 38]. Both studies generated good HMF yields, —55.6% and 42.3%, respectively—using water as a
95 conversion solvent. In addition, other studies have used glucose as a feedstock: Zou et al. used bagasse-
96 based activated carbon and sulfonated it with sulfuric acid, while Villanueva et al. used carboxylated
97 activated carbon [39, 40]. However, both studies produced low HMF yields: 10%, at 130 °C in 8 hours; and <
98 5%, at 125 °C in 3 hours, respectively. Meanwhile, Tyagi et al. combined Brønsted and Lewis acid sites in the
99 same carbon catalyst by impregnating metals into sulfuric acid-treated activated carbon [41]. These
100 researchers were able to produce a 49% HMF yield using cellulose as feedstock and an ionic liquid as a
101 reaction medium. In this work, AC produced from birch sawdust was modified with ZnCl₂ or H₂SO₄ to create
102 Lewis or Brønsted acid sites, respectively, on the AC surface. The objective was then to study the
103 effectiveness of prepared heterogeneous AC catalysts in the conversion of glucose to HMF in biphasic
104 water:THF system. The reaction conditions were studied in detail to find optimal catalyst loading and
105 reaction time. Furthermore, the recyclability of the catalyst containing water phase was studied with some
106 preliminary experiments.

107



109

110 **Figure 1.** General reaction scheme of HMF formation from glucose. First, glucose is isomerized into fructose
111 over a Lewis acid catalyst, and then fructose is dehydrated into HMF over a Brønsted acid catalyst.

111

112 2. Experimental

113

114 2.1 Materials

115

116 All chemicals in this work were commercially available and were used without further purification. Birch
117 sawdust (*Betula pendula*) was received from a sawmill in Northern Sweden.

118

119 2.2 Activated carbon support and catalyst preparation

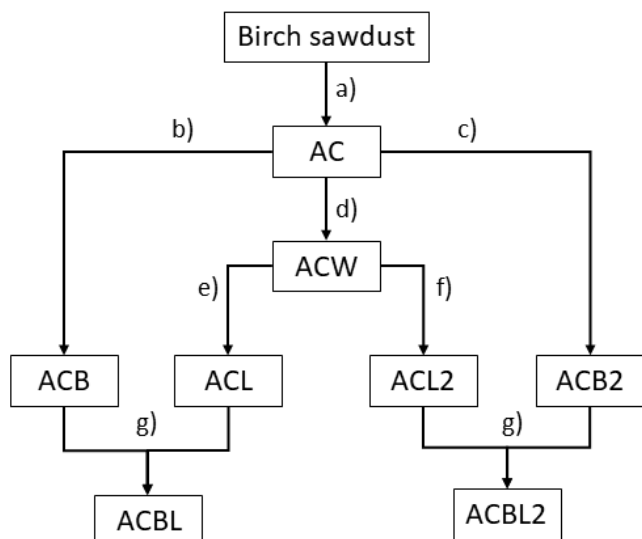
120

121 Activated carbon was produced from birch sawdust. The sawdust was dried, carbonized and steam-
122 activated in a one-step process in a rotating quartz reactor (Nabertherm GmbH RSRB 80). The thermal
123 profile during the process was divided into two parts. In the carbonization step, which was performed
124 under an N₂ flow (200 ml/min), the temperature was raised to 800 °C with a ramp of 6.7 °C/min. During the
125 activation, the temperature was kept at 800 °C for 120 minutes with a stream of water steam and N₂ gas
126 (120 g/h at 140 °C and 200 ml/min, respectively). The resulting activated carbon (AC, Figure 2) was crushed
127 and sieved to a fraction size of < 150 µm. Finally, it was either washed with hot water (ACW, Figure 2) or
128 used as such for further modification.

129

130 Modified solid acid catalysts were prepared by the reflux method from AC or the impregnation
131 method from ACW. To introduce Brønsted acid sites on the activated carbon surface, untreated AC was
132 heated in reflux system at 80 °C for 2 hours with 9 M or 18 M H₂SO₄ (ACB or ACB2, Figure 2). The amount of
133 acid was 10 mL per g of AC. After acid treatment, ACBs were filtered and washed with distilled water until
134 the pH of the filtrate was neutral; lastly, the ACBs were dried overnight at 105 °C. Dried ACBs were
135 extracted in boiling toluene for 2 hours in order to remove unreacted sulfuric acid, after which they were
136 water-washed and then dried overnight at 105 °C [42]. To introduce Lewis acid sites on the ACW surface,
137 catalysts were prepared by incipient-wetness impregnation method [43-44] of a precursor salt, ZnCl₂, and
138 selected to contain nominal 5 wt.% or 15 wt.% of zinc (ACL and ACL2, respectively, Figure 2). Impregnation
139 was performed overnight in a rotating mixer (Rotavapor) at room temperature. After impregnation, the
140 catalysts were dried overnight at 105 °C. The thermal calcination treatment was performed in a chemical
141 vapor deposition (CVD) oven at 550 °C for 2.5 hours with an N₂ flow (240 ml/h per g of catalyst). In addition,
142 two catalytic mixtures, ACBL and ACBL2, were made by combining equal amounts of ACB and ACL or ACB2
143 and ACL2, respectively (Figure 2).

143



144
145
146
147
148
149

Figure 2. Flow chart for catalyst preparation: a) carbonization and activation step b) acid modification with 9 M H₂SO₄ c) acid modification with 18 M H₂SO₄ d) washing with H₂O e) impregnation with ZnCl₂ (5 wt.% Zn) f) impregnation with ZnCl₂ (15 wt.% Zn) g) mixing in 1:1 ratio.

150
151

2.3 Characterization of catalysts

152
153
154
155
156
157
158

The morphology of the catalyst particles was studied using a JEOL JEM-2200FS energy filtered transmission electron microscope equipped with a scan generator (EFTEM/STEM). The catalyst samples were dispersed in pure ethanol and pretreated in an ultrasonic bath for several minutes to create a microemulsion. A small drop of the microemulsion was deposited on a copper grid pre-coated with carbon (Lacey/Carbon 200 Mesh Copper) and evaporated in air at room temperature. The accelerating voltage in the measurements was 200 kV, while the resolution of the STEM image was 0.2 nm. The metal particle sizes were estimated from high-resolution STEM images of each sample.

159
160
161
162
163
164

Specific surface areas were calculated from adsorption isotherms of N₂ at isothermal conditions in liquid nitrogen according to the Brunauer–Emmett–Teller (BET) theory [45]. Pore distribution was calculated from the adsorption isotherms using the density functional theory (DFT) model [46]. The fresh catalyst samples (about 100 mg) were weighted in a quartz tube. Samples were evacuated and heated to 140 °C to remove any adsorbed components as well as to reduce moisture. The measurements were performed by a Micromeritics ASAP 2020 equipment.

165
166
167
168
169
170
171

The Zn, Na, K, Ca, and S contents of prepared AC and catalysts were measured by ICP-OES using a Perkin Elmer Optima 5300 DV instrument. Samples of 0.1-0.2 g were first digested in a microwave oven (MARS, CEM Corporation) with 9 ml of HNO₃ at 200 °C for 10 minutes. Then, 3 ml of HCl was added, and the mixture was digested at 200 °C for 10 minutes. Finally, 1 ml of HF was added, and the mixture was again digested at 200 °C for 10 minutes. Excess HF was neutralized with H₃BO₃ by heating at 170 °C for 10 minutes. Afterwards, the solution was diluted to 50 ml with water, and the former elements were analyzed by the ICP-OES.

172
173
174
175

X-ray diffractograms were recorded by Rigaku SmartLab 9 kW X-ray diffraction (XRD) equipment using Cu K_α radiation (K_β filtered) at 45 kV and 200 mA. Diffractograms were collected in the 2θ range of 5–100°, with a step size of 0.02° and a scan speed of 4.06 degree/min. The crystalline phases and structures were analyzed by PDXL2 program and PDF-4+ 2018.

176 X-ray photoelectron spectroscopy (XPS) analyses were performed using the Thermo Fisher
177 Scientific ESCALAB 250Xi XPS System. With a pass energy of 20 eV and a spot size of 900 μm , the accuracy
178 of the reported binding energies (BEs) was ± 0.2 eV. The Zn, C, O, S, and N were measured for all samples.
179 The measurement data were analyzed by Avantage software. The monochromatic AlK α radiation (1486.6
180 eV) was operated at 20 mA and 15 kV. Charge compensation of the BEs was performed by applying the C1s
181 line at 284.8 eV as a reference.

182 Temperature programmed desorption (TPD) of NH_3 was performed by an AutoChem II 2920
183 system. Prior to the NH_3 -TPD analysis, the samples (about 100 mg) were pre-treated in an He flow of 50
184 ml/min at 600 $^\circ\text{C}$ for 30 minutes. Afterward, the samples were cooled to 100 $^\circ\text{C}$, and the adsorption of
185 ammonia (50 ml/min of 15% NH_3/He at 100 $^\circ\text{C}$) was continued for 60 minutes. Prior to the desorption, the
186 samples were flushed in an He flow of 50 ml/min for 30 minutes to remove all reversibly adsorbed NH_3 . The
187 NH_3 desorption was carried out from 100 to 800 $^\circ\text{C}$ and left for 10 minutes at this temperature. During the
188 analysis, a temperature ramp of 10 $^\circ\text{C}/\text{min}$ and an He flow rate of 50 ml/min were used. The total amount
189 of acid sites (mmol/g) were calculated.

190

191 **2.4 Conversion of glucose into HMF**

192

193 In a typical reaction, 45 mg (0.25 mmol) of glucose, 0.35 g of NaCl, 1.5-18 mg of catalyst (corresponding to
194 0.4-5.0 μmol of Zn and 0.7-23 mM H_2SO_4), and a magnetic stirring bar were placed into a 5 ml reaction
195 tube. Water (1 ml) and THF (3 ml) were added, and the tube was sealed. The reaction was carried out in a
196 Biotage Initiator microwave reactor at 160 $^\circ\text{C}$ for 30 minutes to 8 hours. After the reaction, a sample was
197 taken from both phases, which were filtered through a 0.45 μm PTFE filter for further analysis. The pH of
198 the water phase was checked before and after the reaction. In the recycling experiments, the organic phase
199 was removed after the reaction, and a new portion of glucose and THF was added to a recycled water
200 phase, which included the catalyst. Recycling continued for five runs. All reactions were duplicated.

201

202 **2.5 Analytical methods**

203

204 High-performance liquid chromatography (HPLC) and gas chromatography (GC) were used as analytical
205 methods to determine the amount of HMF in the reaction solutions. The water phase was analyzed with
206 HPLC, while the organic phase was analyzed with HPLC and GC. HPLC analysis was carried out using a
207 Waters 2695 separation module fitted with an Atlantis T3 (3 μm , 4.6 x 150 mm) column and a Waters 996
208 photodiode array (PDA) detector. A water:methanol (90:10) mixture was used as the mobile phase, with a
209 flow rate of 1 ml/min. The injection volume was 4 μl . The column temperature was kept constant at 30 $^\circ\text{C}$,
210 and the UV detection for HMF was performed at 284 nm. GC analysis was carried out using an HP 6890
211 Series GC system fitted with a Sulpelco SPB-1701 (0.25 μm , 15 m x 0.25 mm) column and an HP 5973 mass
212 selective detector. The oven temperature program was as follows: from 60 $^\circ\text{C}$ (hold 1 min) at 20 $^\circ\text{C}/\text{min}$ to
213 250 $^\circ\text{C}$ (hold 2 min), with the injection and detection temperatures set at 250 $^\circ\text{C}$. Helium was used as a
214 carrier gas, with a flow of 1.5 ml/min. GC-MS was also used to qualitatively determine the byproducts of
215 the conversion reaction. Amounts of byproducts other than levulinic acid were not determined. HMF and
216 LA calibrations were performed using analytical standards (Sigma Aldrich).

217

218 The yield of HMF was calculated from the equation:

219 $Y_{\text{HMF}} (\%) = [\text{concentration of HMF in the sample} / \text{theoretical maximum concentration of HMF in the}$
220 $\text{sample}] \times 100\%$

221

222 The yield of LA was calculated using the same principle.

223

224 To determine the reaction selectivity, the amount of glucose from water phase was measured after the
225 conversion reaction. Glucose was measured with YSI 2700 Select Biochemistry Analyzer with glucose
226 solution (2.5 g/l) as a standard. The selectivity of HMF production was then calculated using the following
227 equation:

228 $\text{Selectivity (\%)} = [\text{moles of HMF produced} / (\text{moles of glucose at the beginning} - \text{moles of glucose after the}$
229 $\text{reaction})] \times 100\%$

230

231

232 **3. Results and discussion**

233

234 **3.1 Characterization of catalysts**

235

236 AC catalysts prepared in this work were ACW, two Lewis acid catalysts (ACL and ACL2), and two Brønsted
237 acid catalysts (ACB and ACB2). Prepared catalysts were characterized with multiple characterization
238 techniques to verify their catalytic composition, morphology, and surface properties, e.g., surface areas,
239 active metal phases, and functional groups.

240 Catalyst morphology was observed with transmission electron microscope (EFTEM/STEM). From
241 STEM images (Fig. S1), no major differences in the surface composition were detected when the ACW
242 surface was compared to the surfaces of ACB and ACB2. Instead, on Lewis acid catalysts (ACL and ACL2)
243 prepared from ZnCl_2 , metal particles were clearly seen and evenly distributed on the surface of the catalyst.
244 Metal particle sizes in both ACL and ACL2 catalyst were ca. 10–50 nm; however, some metal aggregations
245 around 100 nm were also detected on both catalysts.

246 Specific BET surface areas, average pore volumes, and pore size distributions of the prepared AC
247 support and catalysts were calculated from nitrogen adsorption isotherms by the BET and DFT methods
248 (Table S1). AC had a BET surface area of $800 \text{ m}^2/\text{g}$. The pore volumes were ca. $0.5 \text{ cm}^3/\text{g}$ with mesopore (2–
249 50 nm) volumes of 52% according to the DFT model. Moreover, all catalysts had high BET surface areas,
250 from 560 to $860 \text{ m}^2/\text{g}$, with high mesoporous volumes, which are usually preferred in catalytic systems. The
251 mesoporous structure was preferred, since smaller pores can easily be blocked, especially in the liquid
252 phase. Chemical modification of the AC support with concentrated sulfuric acid seemed to have an impact
253 on the surface pore composition. The treatment opened mesoporous structure of the AC surface.

254 Therefore, there was a 20% increase in the mesopore volumes and a decrease in micropore volumes in
255 ACB2 compared to AC. As the result, the surface area decreased to $700 \text{ m}^2/\text{g}$ (Table S1). When AC was
256 treated with 9 M H_2SO_4 , both surface area and meso and micropore volumes decreased (ACB, Table S1).
257 This might be due to some pore blocking or the addition of functional groups into the pores. To prepare
258 ACW catalyst AC was washed with water, which did not alter the surface area or the meso and micropore
259 volumes considerably (Table S1). However, when ACW was further impregnated with zinc precursor, the
260 surface areas and pore volumes decreased slightly, ca. 3–5% compared to ACW (ACL and ACL2, Table S1).
261 This indicated that metal was present in the pores and surfaces of the ACL and ACL2 catalysts.

262 The Zn and S contents of the ACW, ACB, ACB2, ACL and ACL2 catalysts were measured with ICP-
263 OES. The nominal active metal contents in ACL and ACL2 were 5 or 15 wt.% of Zn, respectively. However,
264 their Zn contents measured by ICP-OES were similar, 1.7 wt.% for ACL and 1.8 wt.% for ACL2. Therefore, the
265 detected zinc concentrations in catalysts ACL and ACL2 were lower than nominal. It has been proposed in

266 literature that during the heat treatment process, in the temperature range between 400-600 °C, the ZnCl₂
 267 dissociates to Zn and Cl₂. Therefore, the evaporation of Zn and Cl₂ could have occurred, though the
 268 temperature was below the boiling point of ZnCl₂ (b.p.732°C) [47]. Further, reaction of ZnCl₂ into ZnO in the
 269 presence of oxygen can occur [47, 48]. Since no O₂ was present in the inert atmosphere (N₂) of calcination
 270 process, it is possible that Zn was bonded only with the oxygen atoms on the surface of AC. No zinc was
 271 detected in ACB and ACB2 catalysts, however, sulfur was present 0.37 wt.% (ACB) or 0.24 wt.% (ACB2)
 272 indicating the addition of sulfur during the H₂SO₄ treatment. In all catalysts, other impurity metals, e.g., K,
 273 Na, were present in negligible amounts (< 0.2 wt.%). Although some calcium was detected from the ACL
 274 catalysts (< 1 wt.%), in ACBs it was present in negligible amounts (< 0.2 wt.%).

275 Metal phases in the catalysts were observed with XRD (Fig. S2). In all catalysts, the assignments
 276 from carbon (JCPDS file no. 01-082-9929) were detected at 2θ=24.6° and 2θ=43.7°, with broad peaks
 277 indicating the amorphous phase of the carbon. For AC, ACW, ACB, ACL, and ACL2, phase identification was
 278 detected for polymorphic silica (tridymite, SiO₂) according to JCPDS file no. 04-012-1133, with peaks at
 279 2θ=20.5, 21.6, 23.2, 29.9, and 35.8°. In ACB2, no silica was detected with XRD analysis. This indicates that
 280 the treatment with 18 M H₂SO₄ removes most of the metal impurities (e.g., water-soluble metals and silica
 281 originating from biomass) from AC, since no peaks other than the one for carbon were detected from the
 282 ACB2. This was also verified with ICP-OES analysis. For the Lewis acid catalysts, ACL and ACL2, JCPDS file no.
 283 04-004-4531 presented zinc oxide corresponding to ZnO(100), (002), (101), (102), (110), (103), and (112),
 284 with peaks at 2θ=31.7, 34.4, 36.2, 47.5, 56.6, 62.8, and 68.0°, respectively. No ZnCl₂ or metallic Zn⁰ was
 285 detected, which confirms that ZnCl₂ was decomposed or bonded to the oxygen functionalities on the
 286 catalyst surface.

287 XPS was performed to determine the presence and abundance of oxygen- and sulfur-containing
 288 functionalities on the catalyst surface (Table 1). Also, information about the presence and relative oxidation
 289 state of the active metal was collected. For all catalysts, the XPS C1s spectrum revealed a high amount of
 290 carbon functionalities (total C-% from 87 to 96%, see Table 1) on the surface, consisting mainly of carbon-
 291 carbon-type bonds and some carbon-oxygen functionalities. From the O1s pattern (Table 1, Fig. S3), both
 292 ACB and ACB2 catalysts were showing higher atomic percent for oxygen functionalities on the surface
 293 indicating surface oxidation. For ACB2 the oxygen content, ca. 12%, was higher than for ACB (ca. 6%, Table
 294 1). From the O1s pattern, the signal at 531 eV can be assigned to C=O double bonds in carbonyl groups as
 295 well as to S=O double bonds in sulfonic acid groups. The peak at 533 eV can correspond to the single-
 296 bonded oxygen atoms, e.g., from hydroxyl groups of phenol type, or to S-O bonds e.g., in sulfonic acid
 297 groups [49-51]. In addition, the peak at 168 eV in the XPS spectra for S2p (Fig. S4) indicated the presence of
 298 sulfonic acid groups in both ACB and ACB2 [52]. The high-resolution XPS spectra of ACL and ACL2 (Fig. S4)
 299 for Zn2p showed peaks at 1022 eV, corresponding to Zn2p_{3/2}, and at 1045 eV assigned to Zn2p_{1/2}. This
 300 indicated the presence of zinc oxide (Zn²⁺) in the catalysts [53], which was also in accordance with the XRD
 301 analysis. For ACW, the total amount of oxygen groups detected on the surface with XPS O1s scan was about
 302 4%. This indicates the presence of for example carboxylic acid groups, which are common in the surfaces of
 303 activated carbons [27].

304
 305 **Table 1.** Atomic percentages (atom-%) of surface groups based on the XPS analysis from catalysts obtained
 306 *via* binding energies of the C1s, O1s, S2p and Zn2p photoelectrons [32-35].

Sample		ACW	ACB	ACB2	ACL	ACL2
	BE (eV) ^a	% ^b	% ^b	% ^b	% ^b	% ^b
Total C-%	From C1s	95.7	93.4	87.4	95.4	94.5
C- (sp ³)	(284.8 eV)	52.2	49.7	43.0	51.9	50.6

C= (sp ²)	(285.7 eV)	25.2	25.8	26.5	25.6	25.7
C-O	(288.3 eV)	7.7	7.8	9.7	7.4	7.5
C=O	(290.9 eV)	8.1	7.7	6.3	8.0	8.3
π - π^* in aromatic ring	(293.4 eV)	2.6	2.5	2.0	2.5	2.5
Total O-%	From O1s	4.3	6.3	12.4	3.9	4.6
O=	(531 eV)	2.2	1.3	3.7	2.4	3.2
O-	(533 eV)	2.1	4.3	7.6	1.2	1.0
H ₂ O (ads.)	(536 eV)	n.d.	0.6	1.2	0.3	0.4
Total S-%	(168 eV)	n.d.	0.2	0.1	n.d.	n.d.
Total Zn-%	(1022 eV)	n.d.	n.d.	n.d.	0.4	0.6

307 ^a binding energy \pm 0.2 eV

308 ^b % is the relative amount from atom percent of the total sample

309

310 The total amount of acid sites on the surfaces of ACW, ACB, ACB2, ACL and ACL2 was determined
311 by temperature-programmed desorption of ammonia (NH₃-TPD). The position and the area of the
312 desorption peak correlates directly with the acid strength and the acid amount, respectively. The
313 desorption process of ammonia was measured up to 800 °C. From the TPD profiles (Fig. S5) desorption
314 peaks at 700 °C for ACB2 and at 750 °C for ACL and ACL2 were detected. These high-temperature peaks can
315 be attributed to the desorption of NH₃ from strong Brønsted acid sites with strong and broad desorption
316 peak between 500 and 700 °C [54] and from more thermally stable strong Lewis acid sites at higher
317 temperature, respectively [50, 55]. According to NH₃-TPD-performed analysis, ACW might contain some
318 amount of acidic surface groups, up to a total of 0.45 mmol/g, which could originate from oxygen-bearing
319 functionalities, e.g. carboxylic acids, anhydrides, lactones, lactols or phenols which are typical acidic groups
320 on the activated carbon surface [27]. The number of total acid sites introduced into the catalysts was, at
321 highest, 1.32 mmol/g when the AC was modified with 18 M H₂SO₄ (ACB2) and was three times higher than
322 for ACW indicating addition of acidic functionalities on the surface. As expected, treatment with 9 M H₂SO₄
323 did not add acidity as much as the treatment with strong acid. In fact, the acidity of ACB was 0.45 mmol/g,
324 the same as for ACW. It is very likely, that detected sulfur compounds on ACB (see ICP-OES and XPS) were
325 composed from other type of sulfur groups than from acidic sulfonic groups. According to literature, a large
326 number of oxidized functionalities such as phenolic and carboxylic acid groups can be created on the
327 carbon surface during the sulfuric acid treatment [56-59]. This seems to be in line with the results in this
328 study, since measured sulfur content seemed to be relatively low, but acidity was increased (ACB2). I.e. not
329 only sulfonic acids were formed during the H₂SO₄ treatment but also other oxidized functionalities such as
330 acidic phenolic and carboxylic groups, for example, were formed. Treatment with zinc chloride seemed to
331 increase acidity slightly in the ACLs, since metal oxide (ZnO) was present as a Lewis acid site in the catalyst.
332 The acidity determined by NH₃-TPD was slightly higher in ACL (0.75 mmol/g) than in the ACL2 catalyst (0.62
333 mmol/g). However, no significant differences were detected with acid sites in ACL and ACL2, confirming
334 that the catalysts were almost identical.

335 To conclude the catalyst characterization results, ACB and ACB2 had sulfur-containing
336 functionalities on the catalyst surface. Based on the NH₃-TPD analysis, sulfuric acid treatment with
337 concentrated acid increased the acidity of the ACB2 catalyst. However, also other oxidized functionalities
338 than sulfonic acids seemed to be present such as phenol or carboxylic acid groups increasing the acidic sites
339 on the surface. With the characterization of ACL and ACL2, the addition of zinc was detected with STEM and

340 ICP-OES analysis. Further, the metal phase as metal oxide (ZnO) was verified with XRD and XPS. Overall,
341 both Lewis acid catalysts were almost identical, even though, the nominal metal content was different,
342 indicating ZnCl₂ impregnation was not successful at higher loading. In the future, optimization of the
343 preparation method of activated carbon catalysts containing Lewis and Brønsted acid sites still needs work
344 to obtain higher acidic site loading on the catalyst.

345

346 **3.2 Conversion of glucose into HMF**

347

348 Prepared heterogeneous catalysts (ACW, ACB, ACB2, ACL, ACL2, ACBL and ACBL2) were used to convert
349 glucose to HMF in biphasic media consisting of water and THF. A reaction temperature of 160 °C and a time
350 of 8 hours, were chosen based on some preliminary experiments and were kept constant (Table 2). The first
351 reaction was carried out without catalyst and only a 1% HMF yield was obtained, which indicated that the
352 THF/water mixture could not catalyze the reaction by itself and acted only as a solvent (entry 1). Since THF
353 and water are mutually miscible, NaCl was added to the reaction vessel in order to saturate the water
354 phase and separate the layers. In the biphasic system, the produced HMF was extracted into THF *in situ*,
355 hindering contact between HMF and water. This prevented HMF from reacting further into undesired
356 byproducts. However, NaCl has been shown to catalyze HMF production, since the chloride ions enhance
357 the glucose to fructose isomerization step as well as the fructose to HMF dehydration step [60]. Therefore,
358 another reference reaction with NaCl but without any other catalyst was performed, and a HMF yield of
359 35% was achieved (entry 2). The reaction selectivity was only 44%, though. When prepared catalysts were
360 introduced to the reaction system, the HMF yield and the reaction selectivity increased. With ACW the yield
361 increased by 9 percentage units to 44% (entry 3), which was probably due to the acidity of oxygen-
362 containing groups on the surface of the ACW (XPS, Table 1). The reaction selectivity increased to 57%.
363 When ACB, ACB2, ACL or ACL2 were used as the catalyst, the HMF yield increased to 46–49% (entries 4-7),
364 indicating a slight increase compared to NaCl- and ACW-catalyzed reactions. ACB2 and ACL2 produced
365 slightly higher HMF yields than ACB and ACL, but the difference was only 2 percentage units in both cases
366 (entries 4-5 and 6-7). Based on catalyst characterization results, similar HMF yields between ACL and ACL2
367 were reasonable since their metal contents differed only by 0.1 wt.% according to ICP-OES, and 0.2 atom-%
368 according to XPS. Also, similar HMF yields, 46% and 48%, achieved with ACB and ACB2 catalysts,
369 respectively, were supported by the characterization results with XPS. HMF yields achieved with ACB and
370 ACB2 were excellent compared to those described in the literature, where the isomerization step is not
371 usually catalyzed successfully by acid-treated carbon catalysts [61]. It must be noted, though that NaCl was
372 present in the reaction system and most likely took part in the isomerization of glucose to fructose [60].
373 Similar yields between ACB and ACL as well as between ACB2 and ACL2 (difference of only 1 percentage
374 unit, entries 4–7) can also be explained by the effect of NaCl. Since the HMF yields achieved with ACL, ACL2,
375 ACB and ACB2 catalysts were similar, the reaction selectivity was determined only for the reactions
376 performed with ACB2 and ACL2 catalysts. Both catalysts functioned equally resulting in reaction selectivity
377 of 67% (entries 5 and 7), which was 10 percentage units higher than with ACW. This indicated that even if
378 the catalyst modification did not have a strong effect on the HMF yield, it increased the reaction selectivity
379 considerably. However, the selectivity was not affected by whether the catalyst was modified with Lewis or
380 Brønsted acid.

381

382 Creating tandem sites in the same AC catalyst is problematic because, after the sulfonation of AC,
383 impregnating zinc in the catalyst without destroying the oxygen-bearing sulfonic acid groups is challenging,
384 since high temperatures (> 250 °C) during the calcination process can destroy these sulfonic groups [62].
Therefore, two catalytic mixtures, ACBL and ACBL2, were prepared and used in the conversion reaction to

385 introduce Brønsted and Lewis acid functionalities in the reaction system simultaneously. With ACBL as the
 386 catalyst, similar HMF yields (48%, entry 8) as those achieved with the ACB, ACB2, ACL, and ACL2 catalysts
 387 were generated. However, with ACBL2 as the catalyst, the HMF yield increased to 51% (entry 9). Also, the
 388 reaction selectivity increased further to 78% when compared to single acid catalysts ACB2 or ACL2.
 389 Therefore, based on the results, it seems that both Brønsted and Lewis acid sites not only accelerate the
 390 conversion reaction but also affect the reaction selectivity. The increase in HMF yield was not as high as
 391 expected (only 2 percentage units compared to ACL2) but the increase in reaction selectivity was significant
 392 (11 percentage units). In the literature, HMF yields of 63%, 53% and 23.1% and reaction selectivities of 63%,
 393 60% and 24%, respectively, have been achieved in similar reaction media (water/THF/NaCl) with solid TiO₂-
 394 ZrO₂+Amberlyst 70, Sn-Beta with NH₄F and FePO₄ catalysts, respectively [22, 25, 63]. The HMF yield of 51%
 395 achieved in this study is comparable to those obtained in above mentioned studies and HMF selectivity of
 396 78% is notably better compared to those. Also, the studied catalytic mixture was prepared using more
 397 sustainable lignocellulosic waste as a raw material for the catalysts support, thereby increasing the value of
 398 the obtained results.

399 The effect of solvent system was studied with the ACBL2 catalyst, which produced the highest HMF
 400 yield in previous reactions (Table 2). When the reaction was carried out in water, the HMF yield was low:
 401 15% (entry 10). This indicates that although the biphasic system was important the lack of NaCl could have
 402 attributed to the low HMF yield. Therefore, the reaction was repeated using NaCl. However, the HMF yield
 403 was even lower—only 10% (entry 11). Based on GC-MS spectra, it was concluded that notable amount of
 404 levulinic acid (14%) was formed when NaCl was introduced into the reaction and only water was used as
 405 the solvent. In the biphasic reactions, only trace amounts (< 4%) of levulinic acid were detected.

406 Finally, the studied ACB2, ACL2, and ACBL2 catalysts were compared to homogeneous catalysts, in
 407 which the amounts of H₂SO₄ and Zn were similar to those in heterogeneous catalysts. With homogeneous
 408 catalysts the HMF yields as well as the reaction selectivities were lower than with the studied AC-based
 409 catalysts, only 33–37% and 43–47%, respectively (entries 12–14). Low selectivities are consistent with
 410 literature since homogeneous catalysts and NaCl increase the production of soluble humins and humin
 411 precursors [64, 65, 50]. Low HMF yields are also reasonable since the amounts of H₂SO₄ and/or Zn were
 412 very low in homogeneous systems.

413

414 **Table 2.** Results for conversion of glucose to HMF using various catalysts and solutions.

Entry	System	Catalyst	HMF yield (%)	Selectivity (%)
1	water/THF	-	1	-
2	water/THF/NaCl	-	35	44
3	water/THF/NaCl	ACW	44	57
4	water/THF/NaCl	ACB	46	-
5	water/THF/NaCl	ACB2	48	67
6	water/THF/NaCl	ACL	47	-
7	water/THF/NaCl	ACL2	49	67
8	water/THF/NaCl	ACBL	48	-
9	water/THF/NaCl	ACBL2	51	78
10	water	ACBL2	15	-
11	water/NaCl	ACBL2	10	-
12	water/THF/NaCl	H ₂ SO ₄ ^a	37	47
13	water/THF/NaCl	ZnCl ₂ ^b	35	43
14	water/THF/NaCl	H ₂ SO ₄ + ZnCl ₂ ^c	33	45

415 Reaction conditions: 3 mg catalyst, 45 mg glucose, 0.35 g NaCl, 1 ml water, 3 ml THF, 160 °C, 8 h. ^a 1.944
416 mM H₂SO₄ (corresponding to 3 mg ACB2), ^b 0.1158 g/l ZnCl₂ (corresponding to 3 mg ACL2), ^c 0.972 mM
417 H₂SO₄ and 0.0579 g/l ZnCl₂ (corresponding to 3 mg ACBL2).

418

419 The results from the glucose to HMF conversion reactions suggested that activated carbon itself
420 had an important role as a catalyst during the reaction. Based on the catalyst characterizations the
421 amounts of Lewis and Brønsted acid sites were low in heterogeneous catalysts, so it is likely that activated
422 carbon's high specific surface area and oxygen-containing surface groups had an impact on its catalytic
423 activity. These groups might participate in the dehydration reaction of fructose to HMF, while the large
424 surface area of activated carbon may promote the conversion of glucose by increasing contact areas
425 between reactants [26, 29]. Besides this study, there are also several examples in the literature of how the
426 surface of activated carbon plays an important role in catalytic reactions, such as alcohol dehydration [27,
427 66, 67]. However, from the reaction selectivity point of view the values achieved in this study with plain
428 water washed activated carbon were considerably lower than those with acid treated carbon catalysts.

429

430

431 3.2.1 Optimization of reaction time and catalyst loading

432

433 ACBL2 was chosen for optimization experiments because it produced the highest HMF yield compared to
434 the other catalysts (Table 2). The same reaction temperature, 160 °C, and a biphasic water:THF system
435 were used as in previous reactions, but the reaction time and catalyst loading were varied in order to find
436 the optimal reaction conditions for the conversion of glucose to HMF. As shown in Figure 3a, the HMF yield
437 increased from 8% to 51% when the reaction time increased from 1 to 8 hours, respectively. With a longer
438 reaction time, the HMF yield started to decrease, indicating that 8 hours was the optimal time to maximize
439 the yield. In addition, the amount of 1,4-butanediol, which is the degradation product of THF, was observed
440 to increase with the increasing reaction time. However, the most significant increase in the amount of 1,4-
441 butanediol occurred when the reaction time was 10 hours, implying that 8 hours may be the optimal
442 reaction time also regarding the stability of the biphasic system. The amount of levulinic acid did not seem
443 to increase with increasing time, which implied that the biphasic system worked successfully and prevented
444 rehydration of HMF in the organic phase.

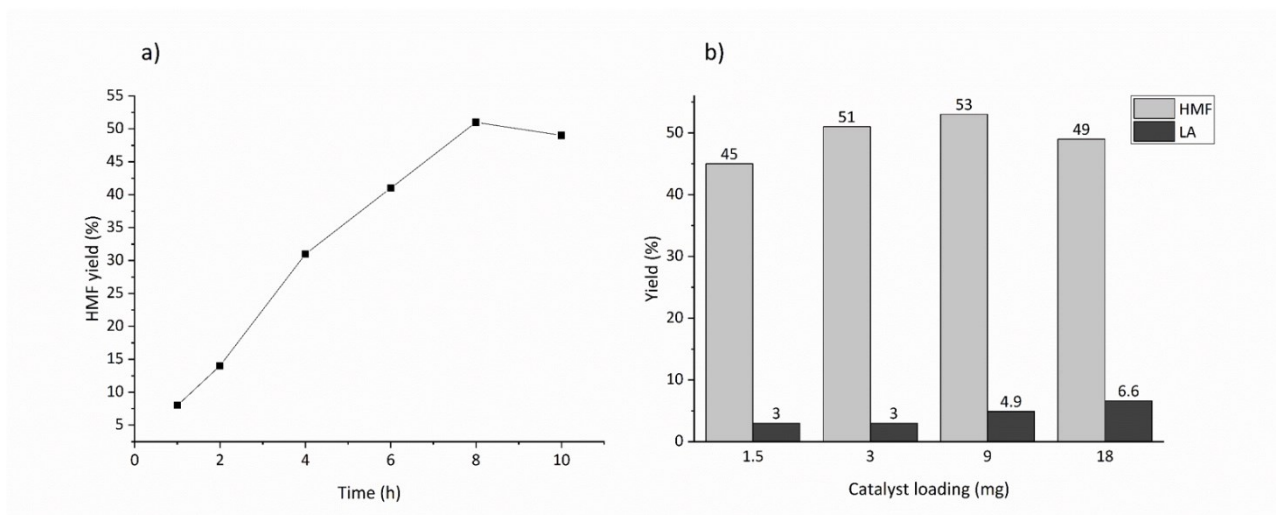
445

446 The amount of catalyst was varied in the range of 1.5–18 mg to determine the optimal catalyst
447 loading. As shown in Figure 3b, the catalyst amount of 1.5 mg was clearly too low to accelerate the
448 conversion reaction, but when the amount was increased to 3 mg, the HMF yield improved significantly,
449 from 45 to 51%. When the catalyst loading was increased to 9 mg, the increase in the HMF yield was only 2
450 percentage units. A further increase in the catalyst amount caused the HMF yield to decrease (Figure 3b),
451 which may be due to the higher amount of Brønsted acid or metal sites in the reaction system, which
452 accelerated side reactions. This was confirmed by measuring levulinic acid concentrations, which increased
453 together with the catalyst loading (Figure 3b). It was also noticed that the formation of 1,4-butanediol in
454 the THF phase was increased with increasing amounts of catalyst. In addition to levulinic acid and 1,4-
455 butanediol, some other unidentified byproducts were formed when the catalyst loading was increased.
456 Thus, 3 mg was selected as the optimal amount of catalyst for the conversion reaction, providing a high
457 yield of HMF with a low amount of byproducts.

457

458

459



460
 461 **Figure 3.** (a) Effect of reaction time on HMF yield. (b) Effect of catalyst loading on HMF and levulinic acid
 462 (LA) yield.

463
 464

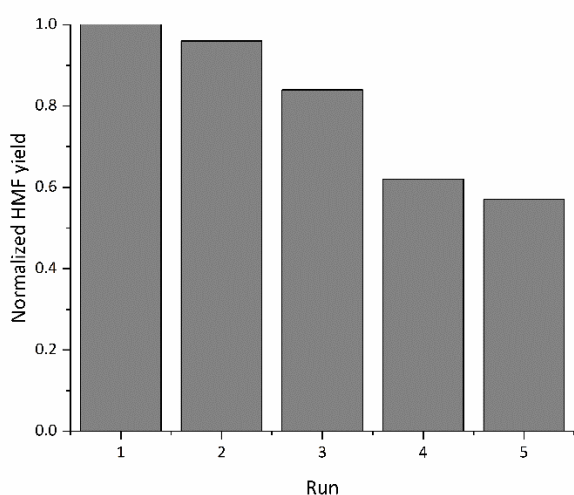
465 3.2.3 Preliminary recycling experiments

466

467 The recyclability of the catalyst is of great importance in the practical production of HMF. In this study, the
 468 catalyst was recycled together with the whole water phase, because the separation of the catalyst would
 469 have significantly reduced the amount of catalyst. The analysis of water phases from previous reactions
 470 revealed that the water phase was suitable for recycling since it did not contain significant amounts of
 471 byproducts: only HMF (yield 5–7%), gamma-butyrolactone and 1,4-butanediol were detected. Also,
 472 unreacted glucose (ca. 34%) was present in the water phase after the conversion reactions, which was
 473 taken into account during the subsequent runs.

474 Recycling was accomplished with an 8-hour reaction time and a 3-mg dosage of ACBL2 catalyst.
 475 After the first reaction the organic phase was removed and analyzed for the HMF yield and a fresh portion
 476 of glucose and THF was added among the water phase for the next run. The results of the recycling
 477 experiments are shown in Figure 4 and based on them the HMF yield decreased after each consecutive run.
 478 However, the decrease in the yield was not significant until after the third run, when it was over 20%. After
 479 that the yield seemed to balance and decreased only slightly between fourth and fifth run. The decrease in
 480 the yield during the recycling experiments could have been caused by adsorption and accumulation of
 481 polymeric side products or humins on the acid sites in the porous catalyst [68]. The composition of the THF
 482 layer did not change notably during the first four runs. After fifth run byproducts such as levulinic acid and
 483 2,3-dihydro-3,5-dihydroxy-6-methyl-4(H)-pyran-4-one [69] were detected with GC-MS. This indicates that
 484 HMF was successfully isolated along with the organic phase between the runs.

485



486

487

Figure 4. The normalized HMF yield after each recycling run in relation to the first run.

488

489

4. Conclusions

490

491

492

493

494

495

496

497

498

499

500

501

502

503

504

505

506

507

508

509

510

511

512

513

514

515

516

517

518

Acknowledgement

The authors acknowledge Davide Bergna for preparing the activated carbon, Seija Liikanen for ICP-OES measurements and Zouhair El Assal for TPD measurements. Also, the Center of Microscopy and Nanotechnology at the University of Oulu is acknowledged for their facilities for STEM/EFTEM imaging and XPS and XRD measurements.

Funding

This work was supported by two projects of the EU/European Regional Development Fund, leveraged from the EU program: project Biomass value chains (no. A71029) and project PreBio (no. A70594). The financial support of EU/Interreg Botnia-Atlantica for project Green Bioraff Solutions (no. 20201508) and Fortum foundation (201700072) is also greatly acknowledged.

Declarations of interest: none.

519 **References**

- 520 [1] S.P. Teong, G. Yi, Y. Zhang, *Green Chem.* 16 (2014) 2015-2026.
- 521 [2] I.K.M. Yu, D.C.W. Tsang, *Bioresour. Technol.* 238 (2017) 716-732.
- 522 [3] T. Wang, M.W. Nolte, B.H. Shanks, *Green Chem.* 16 (2014) 548-572.
- 523 [4] L.T. Mika, E. Cséfalvay, Á Németh, *Chem. Rev.* 118 (2018) 505-613.
- 524 [5] C. Moreau, R. Durand, S. Razigade, J. Duhamet, P. Faugeras, P. Rivalier, R. Pierre, G. Avignon, *Appl. Catal. A Gen.* 145 (1996) 211-224.
- 525
- 526 [6] M.J. Antal, W.S. Mok, G.N. Richards, *Carbohydr. Res.* 199 (1990) 91-109.
- 527 [7] Y. Qu, C. Huang, J. Zhang, B. Chen, *Bioresour. Technol.* 106 (2012) 170-172.
- 528 [8] F.K. Kazi, A.D. Patel, J.C. Serrano-Ruiz, J.A. Dumesic, R.P. Anex, *Chem. Eng. J.* 169 (2011) 329-338.
- 529 [9] Y. Román-Leshkov, J.N. Chheda, J.A. Dumesic, *Science* 312 (2006) 1933-1937.
- 530 [10] J. Zhang, E. Weitz, *ACS Catal.* 2 (2012) 1211-1218.
- 531 [11] J. Lewkowski, *ARKIVOC* 2001 (2005) 17-54.
- 532 [12] B. Saha, M.M. Abu-Omar, *Green Chem.* 16 (2014) 24-38.
- 533 [13] D. Chen, F. Liang, D. Feng, M. Xian, H. Zhang, H. Liu, F. Du, *Chem. Eng. J.* 300 (2016) 177-184.
- 534 [14] R. van Putten, van der Waal, Jan C, E. de Jong, C.B. Rasrendra, H.J. Heeres, J.G. de Vries, *Chem. Rev.*
535 113 (2013) 1499-1597.
- 536 [15] C.J. Moye, *Rev. Pure Appl. Chem.* 14 (1964) 161-170.
- 537 [16] M.S. Feather, J.F. Harris, *Adv. Carbohydr. Chem.* 28 (1973) 161-224.
- 538 [17] P. Bhaumik, P.L. Dhepe, *Catal. Rev.* 58 (2016) 36-112.
- 539 [18] B.Y. Yang, R. Montgomery, *Carbohydr. Res.* 280 (1996) 27-45.
- 540 [19] Y. Yang, C. Hu, M.M. Abu-Omar, *Green Chem.* 14 (2012) 509-513.
- 541 [20] Y.J. Pagán-Torres, T. Wang, J.M.R. Gallo, B.H. Shanks, J.A. Dumesic, *ACS Catal.* 2 (2012) 930-934.
- 542 [21] P.Y. Dapsens, C. Mondelli, J. Pérez-Ramírez, *ACS Catal.* 2 (2012) 1487-1499.
- 543 [22] L. Atanda, A. Silahua, S. Mukundan, A. Shrotri, G. Torres-Torres, J. Beltramini, *RSC Adv.* 5 (2015) 80346-
544 80352.
- 545 [23] X. Wang, H. Zhang, J. Ma, Z. Ma, *RSC Adv.* 6 (2016) 43152-43158.

- 546 [24] J.M.R. Gallo, D.M. Alonso, M.A. Mellmer, J.A. Dumesic, *Green Chem.* 15 (2012) 85-90.
- 547 [25] G. Yang, C. Wang, G. Lyu, L.A. Lucia, J. Chen, *BioResources* 10 (2015) 5863-5875.
- 548 [26] F. Rodríguez-Reinoso, *Carbon* 36 (1998) 159-175.
- 549 [27] J.L. Figueiredo, M.F.R. Pereira, *Catal Today* 150 (2010) 2-7.
- 550 [28] T.J. Bandoz, *Surface Chemistry of Carbon Materials*, in: P. Serp, J.L. Figueiredo (Eds.), *Carbon Materials*
551 *for Catalysis*, John Wiley & Sons, 2008, pp. 45-92.
- 552 [29] E. Lam, J.H.T. Luong, *ACS Catal.* 4 (2014) 3393-3410.
- 553 [30] J.L. Figueiredo, M.F.R. Pereira, M.M.A. Freitas, J.J.M. Órfão, *Carbon* 37 (1999) 1379-1389.
- 554 [31] C. Moreno-Castilla, M.V. López-Ramón, F. Carrasco-Marín, *Carbon* 38 (2000) 1995-2001.
- 555 [32] Y. Yang, K. Chiang, N. Burke, *Catal. Today* 178 (2011) 197-205.
- 556 [33] Anon., Calgon Carbon Corporation Investor Presentation, 2011, [http://phx.corporate-](http://phx.corporate-ir.net/External.File?item=UGFyZW50SUQ9ODc0MjV8Q2hpbGRJRjRD0tMXxUeXBIPtM=&t=1)
557 [ir.net/External.File?item=UGFyZW50SUQ9ODc0MjV8Q2hpbGRJRjRD0tMXxUeXBIPtM=&t=1](http://phx.corporate-ir.net/External.File?item=UGFyZW50SUQ9ODc0MjV8Q2hpbGRJRjRD0tMXxUeXBIPtM=&t=1), accessed 19
558 September 2018.
- 559 [34] M. Danish, T. Ahmad, *Renew. Sust. Energ. Rev.* 87 (2018) 1-21.
- 560 [35] L. Prati, D. Bergna, A. Villa, P. Spontoni, C.L. Bianchi, T. Hu, H. Romar, U. Lassi, *Catal. Today* 301 (2018)
561 239-243.
- 562 [36] P. González-García, *Renew. Sust. Energ. Rev.* 82 (2018) 1393-1414.
- 563 [37] T. Deng, J. Li, Q. Yang, Y. Yang, G. Lv, Y. Yao, L. Qin, X. Zhao, X. Cui, X. Hou, *RSC Adv.* 6 (2016) 30160-
564 30165.
- 565 [38] X. Xiong, I.K.M. Yu, S.S. Chen, D.C.W. Tsang, L. Cao, H. Song, E.E. Kwon, Y.S. Ok, S. Zhang, C.S. Poon,
566 *Catal. Today* 314 (2018) 52-61.
- 567 [39] B. Zou, X. Chen, C. Zhou, X. Yu, H. Ma, J. Zhao, X. Bao, *Can. J. Chem. Eng.* 96 (2018) 1337-1344.
- 568 [40] N.I. Villanueva, T.G. Marzioletti, *Catal. Today* 302 (2018) 100-107.
- 569 [41] U. Tyagi, N. Anand, D. Kumar, *Bioresour. Technol.* 267 (2018) 326-332.
- 570 [42] J.H. Clark, V. Budarin, T. Dugmore, R. Luque, D.J. Macquarrie, V. Strelko, *Catal. Commun.* 9 (2008)
571 1709-1714.
- 572 [43] E. Mäkelä, R. Lahti, S. Jaatinen, H. Romar, T. Hu, R.L. Puurunen, U. Lassi, R. Karinen, *ChemCatChem* 10
573 (2018) 3269-3283.
- 574 [44] R. Lahti, D. Bergna, H. Romar, T. Hu, A. Comazzi, C. Pirola, C.L. Bianchi, U. Lassi, *Top. Catal.* 60 (2017)
575 1415-1428.

- 576 [45] S. Brunauer, P.H. Emmett, E. Teller, *J. Am. Chem. Soc.* 60 (1938) 309-319.
- 577 [46] N.A. Seaton, Walton, J. P. R. B., N. Quirke, *Carbon* 27 (1989) 853-861.
- 578 [47] W.T. Tsai, C.Y. Chang, S.L. Lee, S.Y. Wang, *J. Therm. Anal. Cal.* 63 (2001) 351–357.
- 579 [48] S.A. Schmidt, N. Kumar, A. Shchukarev, K. Eränen, J-P. Mikkola, D.Y. Murzin, T. Salmi, *Appl. Catal., A*
580 468 (2013) 120-134.
- 581 [49] P. Rechnia-Goracy, A. Malaika, M. Kozłowski, *Diamond Relat. Mat.* 87 (2018) 124-133.
- 582 [50] P.P. Upare, J. Yoon, M.Y. Kim, H. Kang, D.W. Hwang, Y.K. Hwang, H.H. Kung, J. Chang, *Green Chem.* 15
583 (2013) 2935-2943.
- 584 [51] P. Burg, P. Fydrych, D. Cagniant, G. Nanse, J. Bimer, A. Jankowska, *Carbon* 40 (2002) 1521-1531.
- 585 [52] Q. Shu, J. Gao, Z. Nawaz, Y. Liao, D. Wang, J. Wang, *Appl. Energy* 87 (2010) 2589-2596.
- 586 [53] C.H. Kim, B.H. Kim, *J. Power Sources.* 274 (2015) 512-520.
- 587 [54] M. Farabi, M. Ibrahim, U. Rashid, Y. Taufiq-Yap, *Energy Convers. Manag.* 181 (2019) 562-570.
- 588 [55] F. Lónyi, J. Valyon, *Micropor. Mesopor. Mater.* 47 (2001) 293-301.
- 589 [56] J. Wang, W. Xu, J. Ren, X. Liu, G. Lua, Y. Wang, *Green Chem.* 13 (2011) 2678-2681.
- 590 [57] S. Kang, J. Ye, Y. Zhanga, J. Chang, *RSC Adv.* 3 (2013) 7360-7366.
- 591 [58] H.T. Gomes, S.M. Miranda, M.J. Sampaio, J.L. Figueiredo, A.M.T. Silva, J.L. Faria, *Appl. Catal. B: Environ.*,
592 106 (2011) 390-397.
- 594 [59] X. Xiong, I.K.M. Yu, S.S. Chen, D.C.W. Tsang, L. Cao, H. Song, E.E. Kwon, Y.S. Ok, S. Zhang, C.S. Poon,
595 *Catal. Today*, 314 (2018) 52-61.
- 596 [60] X. Li, Y. Zhang, Q. Xia, X. Liu, K. Peng, S. Yang, Y. Wang, *Ind. Eng. Chem. Res.* 57 (2018) 3545-3553.
- 597 [61] W. Daengprasert, P. Boonnoun, N. Laosiripojana, M. Goto, A. Shotipruk, *Ind. Eng. Chem. Res.* 50 (2011)
598 7903-7910.
- 599 [62] Q. Pang, L. Wang, H. Yang, L. Jia, X. Pan, C. Qiu, *RSC Adv.* 4 (2014) 41212-41218.
- 600 [63] L. Yang, X. Yan, S. Xu, H. Chen, H. Xia, S. Zuo, *RSC Adv.* 5 (2015) 19900-19906.
- 601 [64] V. Maruani, S. Narayanin-Richenapin, E. Framery, B. Andrioletti, *ACS Sustainable Chem. Eng.* 6 (2018)
602 13487-13493.
- 603 [65] I.K.M Yu, D.C.W Tsang, *Bioresour. Technol.* 238 (2017) 716-732.
- 604 [66] Q.X. Lin, C.H. Zhang, X.H. Wang, B.G. Cheng, N. Mai, J.L. Ren, *Catal. Today* (2018) Article in press.
- 605 [67] S.S. Chen, T. Maneerung, D.C.W. Tsang, Y.S. Ok, C.H. Wang, *Chem. Eng. J.* 328 (2017) 246-273.

606 [68] A. Deng, Q. Lin, Y. Yan, H. Li, J. Ren, C. Liu, R. Sun, *Bioresour. Technol.* 216 (2016) 754-760.

607 [69] M. Kim, W. Baltes, *J. Agric. Food Chem.* 44 (1996) 282-289.

608